

Westinghouse Non-Proprietary Class 3

WCAP-16020-NP
Revision 0

February 2003

Technical Justification for Eliminating 12" Residual Heat Removal (RHR) Lines Rupture as the Structural Design Basis For Callaway Nuclear Power Plant



WCAP-16020-NP Revision 0

**Technical Justification for Eliminating
12" Residual Heat Removal (RHR) Lines Rupture as
the Structural Design Basis for
Callaway Nuclear Power Plant**

D. C. Bhowmick
C. K. Ng

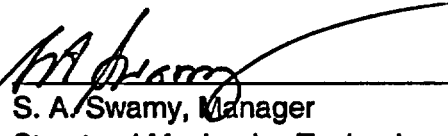
February 2003

Verified:


J. F. Petsche

Structural Mechanics Technology

Approved:


S. A. Swamy, Manager
Structural Mechanics Technology

Westinghouse Electric Company LLC
P.O. Box 355
Pittsburgh, PA 15230-0355

© 2003 Westinghouse Electric Company LLC
All Rights Reserved

TABLE OF CONTENTS

LIST OF TABLES.....	v
LIST OF FIGURES	vi
1 INTRODUCTION	1-1
1.1 Background	1-1
1.2 Scope and Objective	1-1
1.3 References	1-2
2 OPERATION AND STABILITY OF THE RHR LINES.....	2-1
2.1 Stress Corrosion Cracking.....	2-1
2.2 Water Hammer	2-2
2.3 Low Cycle and High Cycle Fatigue	2-2
2.4 Other Possible Degradation During Service of the RHR Lines	2-2
3 MATERIAL CHARACTERIZATION.....	3-1
3.1 Pipe Materials And Weld Process.....	3-1
3.2 Material Properties	3-1
3.3 Reference.....	3-1
4 LOADS FOR FRACTURE MECHANICS ANALYSIS	4-1
4.1 Nature of the Loads.....	4-1
4.2 Loads for Crack Stability Analysis.....	4-2
4.3 Loads for Leak Rate Evaluation.....	4-2
4.4 Summary of Loads and Geometry for the RHR Lines.....	4-2
4.5 Governing Locations for the RHR Lines	4-3
5 FRACTURE MECHANICS EVALUATION	5-1

5.1	Global Failure Mechanism.....	5-1
5.2	Leak Rate Predictions	5-2
5.2.1	General Considerations	5-2
5.2.2	Calculation Method	5-2
5.2.3	Leak Rate Calculations.....	5-3
5.3	Stability Evaluation	5-4
5.4	References.....	5-4
6	ASSESSMENT OF FATIGUE CRACK GROWTH	6-1
6.1	Introduction	6-1
6.2	Critical Location For Fatigue Crack Growth Analysis	6-1
6.3	Design Transients.....	6-1
6.4	Stress Analysis	6-1
6.5	OBE Loads.....	6-2
6.6	Total Stress For Fatigue Crack Growth.....	6-2
6.7	Fatigue Crack Growth Analysis.....	6-2
6.7.1	Analysis Procedure.....	6-2
6.8	Results	6-5
6.9	References.....	6-5
7	ASSESSMENT OF MARGINS	7-1
8	CONCLUSIONS.....	8-1
	APPENDIX A - LIMIT MOMENT.....	A-1

LIST OF TABLES

Table 3-1 : Room Temperature Material Properties for the RHR Lines.....	3-2
Table 3-2 : Representative Tensile Properties for the RHR Lines at Operating Temperatures.....	3-2
Table 3-3 : Modulus of Elasticity (E) for the RHR Lines.....	3-2
Table 4-1 : Summary of Callaway Nuclear Power Plant Piping Geometry and Normal Operating Condition for the Residual Heat Removal Line Loop 1	4-4
Table 4-2 : Summary of Callaway Normal Loads and Stresses for Residual Heat Removal Line Loop 1	4-5
Table 4-3 : Summary of Callaway Nuclear Power Plant Faulted Loads and Stresses for Residual Heat Removal Line Loop 1	4-6
Table 4-4 : Summary of Callaway Nuclear Power Plant Piping Geometry and Normal Operating Condition for Residual Heat Removal Line Loop 4	4-7
Table 4-5 : Summary of Callaway Nuclear Power Plant Normal Loads and Stresses for Residual Heat Removal Line Loop 4	4-8
Table 4-6 : Summary of Callaway Nuclear Power Plant Faulted Loads and Stresses for Residual Heat Removal Line Loop 4	4-9
Table 5-1 : Leakage Flaw Sizes	5-5
Table 5-2 : Summary of Critical Flaw Sizes.....	5-5
Table 6-1 : Design Transients Considered for Fatigue Crack Growth Evaluation	6-6
Table 6-2 : RHR Lines Fatigue Crack Growth Results	6-7
Table 7-1 : Leakage Flaw Sizes, Critical Flaw Sizes and Margins.....	7-2
Table 7-2 : LBB Conservatism	7-2

LIST OF FIGURES

Figure 3-1	Callaway Nuclear Power Plant RHR Line Loop 1 Layout	3-3
Figure 3-2	Callaway Nuclear Power Plant RHR Line Loop 4 Layout	3-4
Figure 4-1	Governing Weld Location for RHR Line Loop 1	4-10
Figure 4-2	Governing Weld Location for RHR Line Loop 4	4-11
Figure 5-1	Fully Plastic Stress Distribution	5-6
Figure 5-2	Analytical Predications of Critical Flow Rates of Steam-Water Mixtures	5-7
Figure 5-3	[] ^{a,c,e} Pressure Ratio as a Function of L/D	5-8
Figure 5-4	Idealized Pressure Drop Profile through a Postulated Crack	5-9
Figure 5-5	Loads acting on the Model at the Governing Locations	5-10
Figure 5-6	Critical Flaw Size Prediction for Node 3020 (RHR Line Loop 4)	5-11
Figure 5-7	Critical Flaw Size Prediction for Node 3285 (RHR Line Loop 1)	5-12
Figure 6-1	Schematic of RHR Line at RCL Hot Leg Nozzle Weld Location	6-8
Figure 6-2	Reference Crack Growth Curves for Stainless Steel in Air Environments	6-9
Figure A-1	Pipe with A Through-Wall Crack in Bending	A-2

1 INTRODUCTION

1.1 BACKGROUND

The current structural design basis for the Residual Heat Removal (RHR) lines requires postulating non-mechanistic circumferential and longitudinal pipe breaks. This results in additional plant hardware (e.g., pipe whip restraints and jet shields) which would mitigate the dynamic consequences of the pipe breaks. It is, therefore, highly desirable to be realistic in the postulation of pipe breaks for the RHR lines. Presented in this report are the descriptions of a mechanistic pipe break evaluation method and the analytical results that can be used for establishing that a circumferential type of break will not occur within the RHR lines. The evaluations consider that circumferentially oriented flaws cover longitudinal cases.

1.2 SCOPE AND OBJECTIVE

The scope of this report is limited to the high energy Class 1 portion of the RHR lines (primary loop junction to the second isolation valve). A schematic drawing of the piping system is shown in Section 3. The recommendations and criteria proposed in SRP 3.6.3 (Reference 1-2) are used in this evaluation. The criteria and the resulting steps of the evaluation procedure can be briefly summarized as follows:

1. Calculate the applied loads. Identify the location(s) at which the highest faulted stress occurs.
2. Identify the materials and the material properties.
3. Postulate a surface flaw at the governing location. Determine fatigue crack growth. Show that a through-wall crack will not result.
4. Postulate a through-wall flaw at the governing location(s). The size of the flaw should be large enough so that the leakage is assured of detection with margin using the installed leak detection equipment when the pipe is subjected to normal operating loads. Demonstrate that there is a margin of 10 between the calculated leak rate and the leak detection capability.
5. Using maximum faulted loads in the stability analysis, demonstrate that there is a margin of 2 between the leakage size flaw and the critical size flaw.
6. Review the operating history to ascertain that operating experience has indicated no particular susceptibility to failure from the effects of corrosion, water hammer or low and high cycle fatigue.
7. For the materials types used in the Plant, provide representative material properties.

The leak rate is calculated for the normal operating condition. The leak rate prediction model used in this evaluation is an [

]^{a,c,e}. The crack opening area required for calculating the leak rates is obtained by subjecting the postulated through-wall flaw to normal operating loads (Reference 1-3). Surface roughness is accounted for in determining the leak rate through the postulated flaw.

It should be noted that the terms "flaw" and "crack" have the same meaning and are used interchangeably. "Governing location" and "critical location" are also used interchangeably throughout the report.

1.3 REFERENCES

- 1-1 WCAP-7211, Revision 4, "Energy Systems Business Unit Policy and Procedures for Management, Classification, and Release of Information," January 2001.
- 1-2 Standard Review Plan; public comments solicited; 3.6.3 Leak-Before-Break Evaluation Procedures; Federal Register/Vol. 52, No. 167/Friday, August 28, 1987/Notices, pp. 32626-32633.
- 1-3 NUREG/CR-3464, 1983, "The Application of Fracture Proof Design Methods Using Tearing Instability Theory to Nuclear Piping Postulating Circumferential Through Wall Cracks."

2 OPERATION AND STABILITY OF THE RHR LINES

2.1 STRESS CORROSION CRACKING

The Westinghouse Reactor Coolant System (RCS) Class 1 lines have an operating history that demonstrates the inherent operating stability characteristics of the design. This includes a low susceptibility to cracking failure from the effects of corrosion (e.g., intergranular stress corrosion cracking, IGSCC). This operating history totals over 1100 reactor-years, including 5 plants each having over 30 years of operation, 4 plants each with over 25 years of operation, 12 plants each with over 20 years of operation and 8 plants each with over 15 years of operation.

For stress corrosion cracking (SCC) to occur in piping, the following three conditions must exist simultaneously: high tensile stresses, susceptible material, and a corrosive environment. Since some residual stresses and some degree of material susceptibility exist in any stainless steel piping, the potential for stress corrosion is minimized by properly selecting a material immune to SCC as well as preventing the occurrence of a corrosive environment. The material specifications consider compatibility with the system's operating environment (both internal and external) as well as other materials in the system, applicable ASME Code rules, fracture toughness, welding, fabrication, and processing.

The elements of a water environment known to increase the susceptibility of austenitic stainless steel to stress corrosion are: oxygen, fluorides, chlorides, hydroxides, hydrogen peroxide, and reduced forms of sulfur (e.g., sulfides, sulfites, and thionates). Strict pipe cleaning standards prior to operation and careful control of water chemistry during plant operation are used to prevent the occurrence of a corrosive environment. Prior to being put into service, the piping is cleaned internally and externally. During flushes and preoperational testing, water chemistry is controlled in accordance with written specifications. Requirements on chlorides, fluorides, conductivity, and pH are included in the acceptance criteria for the piping.

During plant operation, the reactor coolant water chemistry is monitored and maintained within very specific limits. Contaminant concentrations are kept below the thresholds known to be conducive to stress corrosion cracking with the major water chemistry control standards being included in the plant operating procedures as a condition for plant operation. For example, during normal power operation, oxygen concentration in the RCS Class 1 lines is expected to be in the parts per billion (ppb) range by controlling charging flow chemistry and maintaining hydrogen in the reactor coolant at specified concentrations. Maintaining concentrations of chlorides and fluorides within the specified limits also stringently controls halogen concentrations. This is assured by controlling charging flow chemistry. Thus during plant operation, the likelihood of stress corrosion cracking is minimized.

Wall thinning by erosion and erosion-corrosion effects will not occur in the RHR lines due to the low velocity, and the material, austenitic stainless steel, is highly resistant to these degradation mechanisms. Therefore, wall thinning is not a significant concern in the portion of the system being addressed in this evaluation.

As a result of the recent issue of Primary Water Stress Corrosion Cracking (PWSCC) occurring in V. C. Summer reactor vessel hot leg nozzle, Alloy 82/182 weld is being currently investigated under the EPRI Materials Reliability Project (MRP) Program. It should be noted that the susceptible material under investigation is not found in the RHR lines at the Callaway Nuclear Power Plant.

2.2 WATER HAMMER

Overall, there is a low potential for water hammer in the RCS and connecting RHR lines since they are designed and operated to preclude the voiding condition in normally filled lines. The RCS and connecting RHR lines including piping and components are designed for normal, upset, emergency, and faulted condition transients. The design requirements are conservative relative to both the number of transients and their severity. Relief valve actuation and the associated hydraulic transients following valve opening are considered in the system design. Other valve and pump actuations are relatively slow transients with no significant effect on the system dynamic loads. To ensure dynamic system stability, reactor coolant parameters are stringently controlled. Temperature during normal operation is maintained within a narrow range by the control rod positions; pressure is controlled also within a narrow range for steady-state conditions by the pressurizer heaters and pressurizer spray. The flow characteristics of the system remain constant during a fuel cycle because the only governing parameters, namely system resistance and the reactor coolant pump characteristics are controlled in the design process. Additionally, Westinghouse has instrumented typical reactor coolant systems to verify the flow and vibration characteristics of the system and the connecting auxiliary lines. Preoperational testing and operating experience has verified the Westinghouse approach. The operating transients of the RCS primary piping and connected RHR lines are such that no significant water hammer can occur.

2.3 LOW CYCLE AND HIGH CYCLE FATIGUE

An assessment of the low cycle fatigue loading is discussed in Section 6 as part of this study in the form of a fatigue crack growth analysis.

Pump vibrations during operation would result in high cycle fatigue loads in the piping system. During operation, an alarm signals the exceedance of the RC pump shaft vibration limits. Field measurements have been made on the reactor coolant loop piping in a number of plants during hot functional testing. Stresses in the elbow below the RC pump have been found to be very small, between 2 and 3 ksi at the highest. Field measurements on typical PWR plants indicate vibration amplitudes less than 1 ksi. When translated to the connecting RHR lines, these stresses would be even lower, well below the fatigue endurance limit for the RHR line materials and would result in an applied stress intensity factor below the threshold for fatigue crack growth.

2.4 OTHER POSSIBLE DEGRADATION DURING SERVICE OF THE RHR LINES

Thermal stratification occurs when conditions permit hot and cold layers of water to exist simultaneously in a horizontal pipe. This can result in significant thermal loadings due to the

high fluid temperature differentials. Changes in the stratification state result in thermal cycling, which can cause fatigue damage. This was an important issue in PWR feedwater line and pressurizer surge line piping, where temperature differentials of 300°F were not uncommon.

For the RHR piping in the Callaway Nuclear Power Plant, thermal stratification is not a concern during normal plant operation, since the unisolable piping extending from the hot leg to the isolation valve is relatively short. This ensures that turbulent penetration from the hot leg will heat the piping and preclude stratification. In addition, thermal stratification is also not a concern during RHR operation, since the flow rate is sufficiently high to preclude stratification.

The RHR Lines and the associated fittings for Callaway Nuclear Power Plant are forged product forms, which are not susceptible to toughness degradation due to thermal aging.

The maximum normal operating temperature of the RHR piping is about 619°F. This is well below the temperature that would cause any creep damage in stainless steel piping.

3 MATERIAL CHARACTERIZATION

3.1 PIPE MATERIALS AND WELD PROCESS

The material types of the RHR lines for the Callaway Nuclear Power Plant are SA376 TP304, SA312 TP304 and SA403 WP304 . They are wrought product of the types used for the piping in several PWR plants. The RHR line system does not include any cast pipes or cast fittings. The welding processes used are Gas Tungsten Arc Weld (GTAW) and Shielded Metal Arc Weld (SMAW) combination or GTAW. Figures 3-1 and 3-2 show the schematic layout of the RHR lines Loop 1 and 4 respectively and also identify the weld location by node points.

In the following sections the tensile properties of the materials are presented for use in the Leak-Before-Break analyses.

3.2 MATERIAL PROPERTIES

The room temperature mechanical properties of the Callaway Nuclear Power Plant RHR lines material were obtained from the Certified Materials Test Reports (CMTRs) and are given in Table 3-1. The material properties at temperatures (70°F and 619°F) are required for the leak rate and stability analyses. The minimum and average tensile properties at the temperatures of interest stated above were calculated by using the ratio of the ASME Code Section II (Reference 3-1) properties and those tabulated in Table 3-1. Table 3-2 shows the representative minimum and average tensile properties at various operating temperatures. The modulus of elasticity values was established at various temperatures from the ASME Code Section II (see Table 3-3). In the Leak-Before-Break evaluation, the representative minimum yield and minimum ultimate strengths at operating temperature were used for the flaw stability evaluations and the representative average yield strength properties were used for the leak rate predictions. These properties are summarized in Table 3-2.

3.3 REFERENCE

- 3-1 ASME Boiler and Pressure Vessel Code Section II, Part D – Material Properties, 2001 Edition, July 1, 2001, ASME Boiler and Pressure Vessel Committee, Subcommittee on Materials.

Table 3-1 : Room Temperature Material Properties for the RHR Lines

Heat No. (S/N)*	Material	Yield Strength (psi)	Ultimate Strength (psi)
L3384 (348)	SA376 TP304	41200	81100
ERLG (441)	SA403 WP304	37860	80730
EROD (437)	SA403 WP304	37440	82630
J6346 (348)	SA376 TP304	42400	84900
ERLG (439)	SA403 WP304	37860	80730
6473 (782)	SA376/SA312 TP304	40300	84500
D9711 (790)	SA403 WP304	36800	81300
D9553 (784)	SA403 WP304	40200	84700
5-621 (451)	SA312 TP304	43200	89300
J6346 (449)	SA376 TP304	42400	84900

*S/N : Serial Number

Table 3-2 : Representative Tensile Properties for the RHR Lines at Operating Temperatures

Material	Temperature (°F)	Minimum Yield (psi)	Average Yield (psi)	Minimum Ultimate (psi)
SA376/SA312 TP304 or SA403 WP304	619	22384	24310	68244
SA376/SA312 TP304 or SA403 WP304	70	36800	39966	80730

Table 3-3 : Modulus of Elasticity (E) for the RHR Lines

Temperature (°F)	E (10 ⁶ psi)
619	25.205
70	28.300

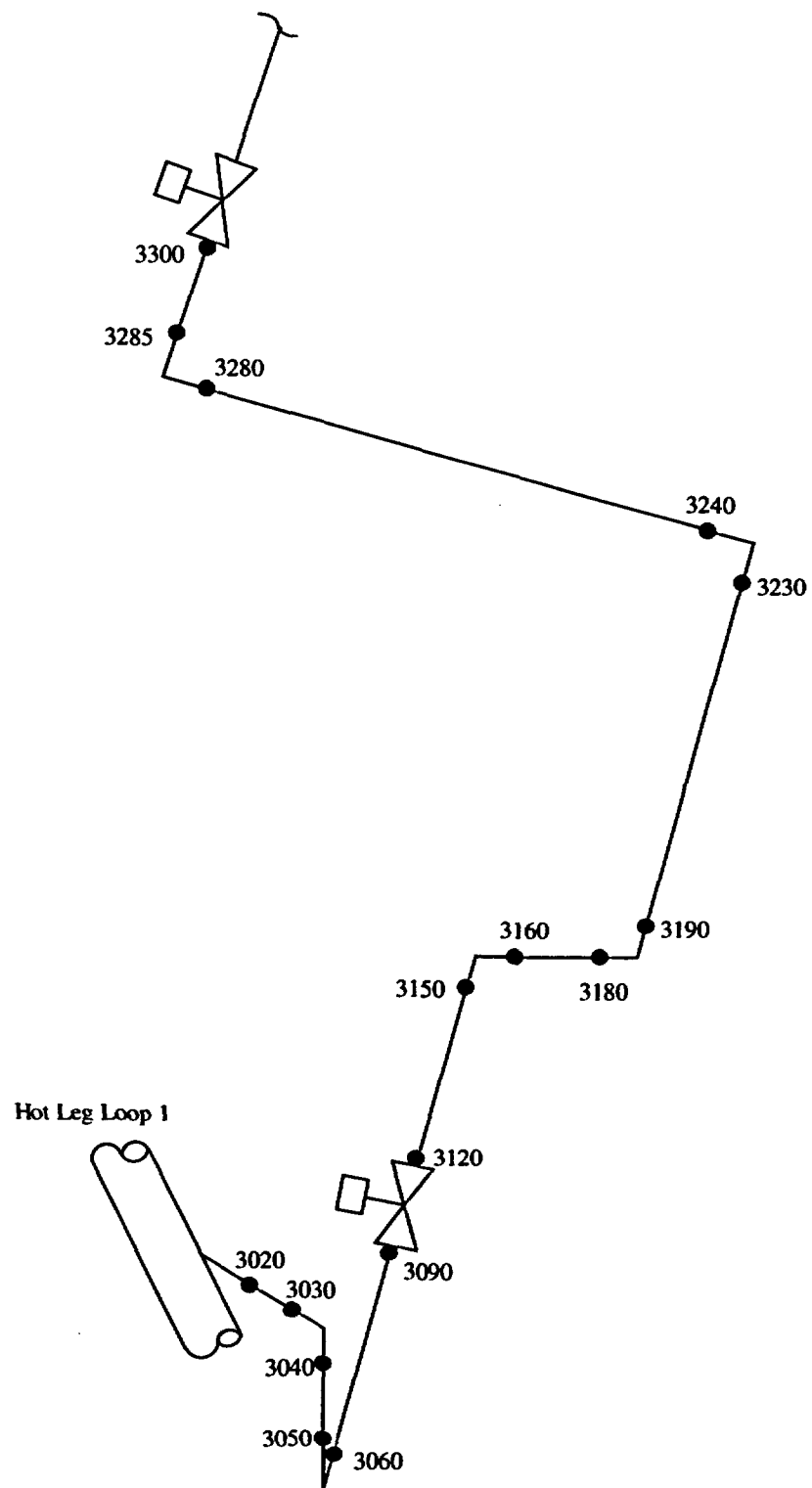


Figure 3-1 Callaway Nuclear Power Plant RHR Line Loop 1 Layout

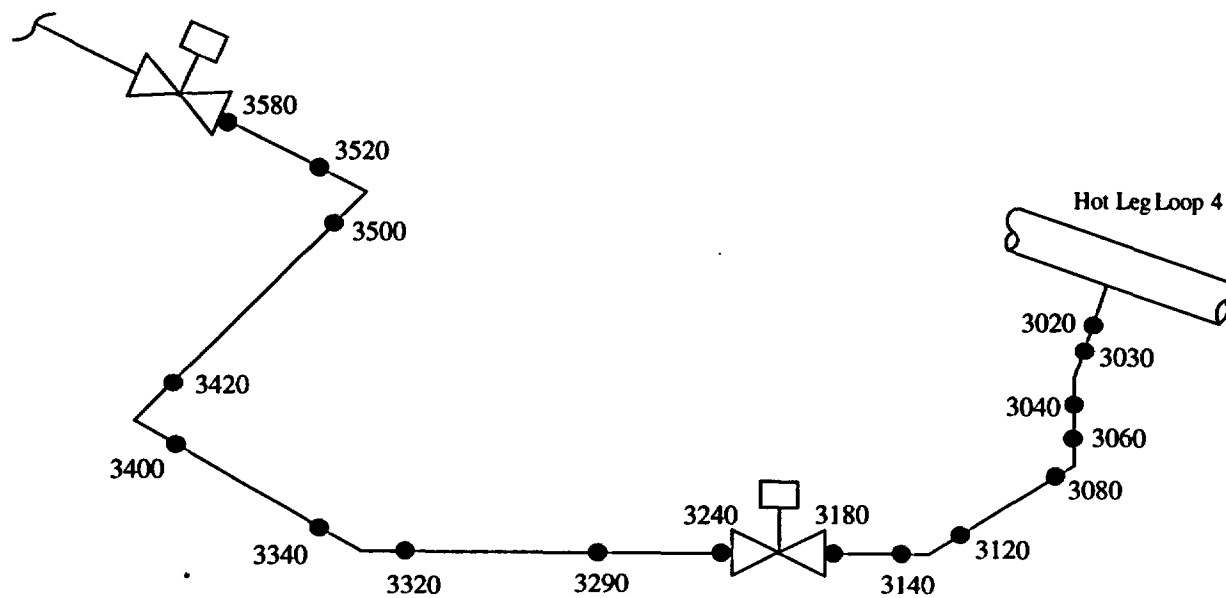


Figure 3-2 Callaway Nuclear Power Plant RHR Line Loop 4 Layout

4 LOADS FOR FRACTURE MECHANICS ANALYSIS

4.1 NATURE OF THE LOADS

Figure 3-1 and Figure 3-2 show schematic layouts of the RHR lines Loop 1 and Loop 4 respectively for Callaway Nuclear Power Plant and identify the weld locations by node points. The stresses due to axial loads and moments were calculated by the following equation:

$$\sigma = \frac{F}{A} + \frac{M}{Z} \quad (4-1)$$

where,

σ	=	Stress
F	=	Axial Load
M	=	Moment
A	=	Metal Cross-Sectional Area
Z	=	Section Modulus

The moment for the desired loading combination was calculated by the following equation:

$$M = \sqrt{M_x^2 + M_y^2 + M_z^2} \quad (4-2)$$

where,

M	=	Moment For Required Loading
M_x	=	Torsional Moment
M_y	=	Y Component of Bending Moment
M_z	=	Z Component of Bending Moment

The axial load and moments for crack stability analysis and leak rate predictions are computed by the methods to be explained in Sections 4.2 and 4.3.

4.2 LOADS FOR CRACK STABILITY ANALYSIS

In accordance with Standard Review Plan 3.6.3 the absolute sum of loading components can be applied which results in higher magnitude of combined loads. If crack stability is demonstrated using these loads, the LBB margin on loads can be reduced from $\sqrt{2}$ to 1.0. The faulted loads for the crack stability analysis were calculated by the absolute sum method as follows:

$$F = |F_{DW}| + |F_{TH}| + |F_P| + |F_{SSE}| \quad (4-3)$$

$$M_X = |M_{XDW}| + |M_{XTH}| + |M_{XSSE}| \quad (4-4)$$

$$M_Y = |M_{YDW}| + |M_{YTH}| + |M_{YSSE}| \quad (4-5)$$

$$M_Z = |M_{ZDW}| + |M_{ZTH}| + |M_{ZSSE}| \quad (4-6)$$

where

DW = Deadweight

TH = Normal Thermal Expansion Load

P = Load Due To Internal Pressure

SSE = Safe Shutdown Earthquake Loading Including Seismic Anchor Motion

4.3 LOADS FOR LEAK RATE EVALUATION

The normal operating loads for the leak rate predictions were calculated by the algebraic sum method as follows:

$$F = F_{DW} + F_{TH} + F_P \quad (4-7)$$

$$M_X = M_{XDW} + M_{XTH} \quad (4-8)$$

$$M_Y = M_{YDW} + M_{YTH} \quad (4-9)$$

$$M_Z = M_{ZDW} + M_{ZTH} \quad (4-10)$$

The parameters and subscripts are the same as those explained in Sections 4.1 and 4.2.

4.4 SUMMARY OF LOADS AND GEOMETRY FOR THE RHR LINES

The load combinations were evaluated at the various weld locations. Normal loads were determined using the algebraic sum method whereas the faulted loads were combined using the absolute sum method. The normal operating loadings for the RHR lines are Pressure (P), Deadweight (DW) and Normal Operating Thermal Expansion (TH) loads. The faulted loadings

consist of Normal Operating loads plus Safe Shutdown Earthquake (SSE) loads including the Seismic Anchor Motion.

Tables 4-1 and 4-4 show the piping geometry and normal operating condition for the RHR lines Loop 1 and Loop 4 at the weld locations respectively. The minimum pipe wall thickness at the weld counterbore is used in the analysis. The normal and faulted loads are tabulated in Tables 4-2 and 4-3 respectively at the weld locations for RHR Line Loop 1, while Tables 4-5 and 4-6 show the normal and faulted loads for RHR Line Loop 4.

4.5 GOVERNING LOCATIONS FOR THE RHR LINES

All the welds at the RHR lines Loops 1 and 4 are fabricated using the GTAW/SMAW combination or GTAW weld process procedures. The governing locations were established on the basis of the pipe schedules, material type, operating temperature, operating pressure, and the highest faulted stresses at the welds. Figures 4-1 and 4-2 show the schematic layouts of the RHR lines Loop 1 and Loop 4 respectively for the Callaway Nuclear Power Plant and also identify the governing weld locations.

The governing locations enveloping both RHR lines Loop 1 and Loop 4 are found to be:

Node 3285 (RHR Line Loop 1)

Node 3020 (RHR Line Loop 4)

Table 4-1 : Summary of Callaway Nuclear Power Plant Piping Geometry and Normal Operating Condition for the Residual Heat Removal Line Loop 1

Weld Location Node	Material Type	Outer Diameter (in)	Minimum Wall Thickness (in)	Normal Operating	
				Pressure (psig)	Temperature (°F)
3020	SA376/SA312 TP304 or SA403 WP304	12.750	1.005	2235	619
3030	SA376/SA312 TP304 or SA403 WP304	12.750	1.005	2235	619
3040	SA376/SA312 TP304 or SA403 WP304	12.750	1.005	2235	619
3050	SA376/SA312 TP304 or SA403 WP304	12.750	1.005	2235	619
3060	SA376/SA312 TP304 or SA403 WP304	12.750	1.005	2235	619
3090	SA376/SA312 TP304 or SA403 WP304	12.750	1.005	2235	619
3120	SA376/SA312 TP304 or SA403 WP304	12.750	1.005	2235	70
3150	SA376/SA312 TP304 or SA403 WP304	12.750	1.005	2235	70
3160	SA376/SA312 TP304 or SA403 WP304	12.750	1.005	2235	70
3180	SA376/SA312 TP304 or SA403 WP304	12.750	1.005	2235	70
3190	SA376/SA312 TP304 or SA403 WP304	12.750	1.005	2235	70
3230	SA376/SA312 TP304 or SA403 WP304	12.750	1.005	2235	70
3240	SA376/SA312 TP304 or SA403 WP304	12.750	1.005	2235	70
3280	SA376/SA312 TP304 or SA403 WP304	12.750	1.005	2235	70
3285	SA376/SA312 TP304 or SA403 WP304	12.750	1.005	2235	70
3300	SA376/SA312 TP304 or SA403 WP304	12.750	1.005	2235	70

Table 4-2 : Summary of Callaway Normal Loads and Stresses for Residual Heat Removal Line Loop 1

Weld Location Node	Axial Force (lbs)	Moment (in-lbs)	Axial Stress (psi)	Moment Stress (psi)	Total Stress (psi)
3020	192298	631638	5186	6252	11439
3030	191926	108653	5176	1075	6252
3040	200560	326835	5409	3235	8644
3050	200490	411556	5407	4074	9481
3060	180263	739254	4862	7317	12179
3090	180623	635570	4871	6291	11163
3120	180623	483086	4871	4782	9653
3150	180623	705757	4871	6986	11857
3160	198000	399180	5340	3951	9291
3180	198030	150267	5341	1487	6828
3190	180623	302359	4871	2993	7864
3230	180623	1300822	4871	12876	17748
3240	196572	1020473	5302	10101	15403
3280	196889	1257967	5310	12452	17762
3285	180623	1552056	4871	15363	20234
3300	180623	1406793	4871	13925	18796

Table 4-3 : Summary of Callaway Nuclear Power Plant Faulted Loads and Stresses for Residual Heat Removal Line Loop 1

Weld Location Node	Axial Force (lbs)	Moment (in-lbs)	Axial Stress (psi)	Moment Stress (psi)	Total Stress (psi)
3020	225671	1507098	6086	14918	21004
3030	225238	401425	6075	3973	10048
3040	211708	499102	5710	4940	10650
3050	211667	622861	5709	6165	11874
3060	246376	1204405	6645	11922	18567
3090	243579	948680	6569	9390	15960
3120	235313	636467	6346	6300	12646
3150	233470	882540	6297	8736	15032
3160	210206	487527	5669	4826	10495
3180	210206	262627	5669	2600	8269
3190	231833	452128	6253	4475	10728
3230	226147	1454034	6099	14393	20492
3240	209645	1183939	5654	11719	17373
3280	210139	1410188	5667	13959	19626
3285	228015	1751544	6150	17338	23487
3300	228023	1586801	6150	15707	21857

Table 4-4 : Summary of Callaway Nuclear Power Plant Piping Geometry and Normal Operating Condition for Residual Heat Removal Line Loop 4

Weld Location Node	Material Type	Outer Diameter (in)	Minimum Wall Thickness (in)	Normal Operating	
				Pressure (psig)	Temperature (°F)
3020	SA376/SA312 TP304 or SA403 WP304	12.750	1.005	2235	619
3030	SA376/SA312 TP304 or SA403 WP304	12.750	1.005	2235	619
3040	SA376/SA312 TP304 or SA403 WP304	12.750	1.005	2235	619
3060	SA376/SA312 TP304 or SA403 WP304	12.750	1.005	2235	619
3080	SA376/SA312 TP304 or SA403 WP304	12.750	1.005	2235	619
3120	SA376/SA312 TP304 or SA403 WP304	12.750	1.005	2235	619
3140	SA376/SA312 TP304 or SA403 WP304	12.750	1.005	2235	619
3180	SA376/SA312 TP304 or SA403 WP304	12.750	1.005	2235	619
3240	SA376/SA312 TP304 or SA403 WP304	12.750	1.005	2235	70
3290	SA376/SA312 TP304 or SA403 WP304	12.750	1.005	2235	70
3320	SA376/SA312 TP304 or SA403 WP304	12.750	1.005	2235	70
3340	SA376/SA312 TP304 or SA403 WP304	12.750	1.005	2235	70
3400	SA376/SA312 TP304 or SA403 WP304	12.750	1.005	2235	70
3420	SA376/SA312 TP304 or SA403 WP304	12.750	1.005	2235	70
3500	SA376/SA312 TP304 or SA403 WP304	12.750	1.005	2235	70
3520	SA376/SA312 TP304 or SA403 WP304	12.750	1.005	2235	70
3580	SA376/SA312 TP304 or SA403 WP304	12.750	1.005	2235	70

Table 4-5 : Summary of Callaway Nuclear Power Plant Normal Loads and Stresses for Residual Heat Removal Line Loop 4

Weld Location Node	Axial Force (lbs)	Moment (in-lbs)	Axial Stress (psi)	Moment Stress (psi)	Total Stress (psi)
3020	188245	1086916	5077	10759	15836
3030	188176	1010275	5075	10000	15075
3040	182761	943054	4929	9335	14264
3060	182429	1024057	4920	10137	15057
3080	198995	740120	5367	7326	12693
3120	199422	252751	5378	2502	7880
3140	195789	278387	5280	2756	8036
3180	195789	593462	5280	5874	11155
3240	195789	1461963	5280	14471	19752
3290	195789	916018	5280	9067	14348
3320	195789	711832	5280	7046	12326
3340	196080	698683	5288	6916	12204
3400	196080	415925	5288	4117	9405
3420	205577	286575	5544	2837	8381
3500	205725	342087	5548	3386	8935
3520	196080	502244	5288	4971	10260
3580	196080	605231	5288	5991	11279

Table 4-6 : Summary of Callaway Nuclear Power Plant Faulted Loads and Stresses for Residual Heat Removal Line Loop 4

Weld Location Node	Axial Force (lbs)	Moment (in-lbs)	Axial Stress (psi)	Moment Stress (psi)	Total Stress (psi)
3020	232496	1826562	6270	18080	24351
3030	232422	1640611	6268	16240	22508
3040	230352	1375521	6213	13616	19828
3060	230064	1251847	6205	12391	18596
3080	225199	1180885	6074	11689	17763
3120	222539	617502	6002	6112	12114
3140	228218	676284	6155	6694	12849
3180	227541	922884	6137	9135	15272
3240	217837	1720972	5875	17035	22910
3290	216718	1106202	5845	10950	16795
3320	213289	780396	5752	7725	13477
3340	211071	787249	5693	7793	13485
3400	210422	515809	5675	5106	10781
3420	207383	375105	5593	3713	9306
3500	210476	558188	5677	5525	11202
3520	212149	706602	5722	6994	12716
3580	212194	766821	5723	7590	13313

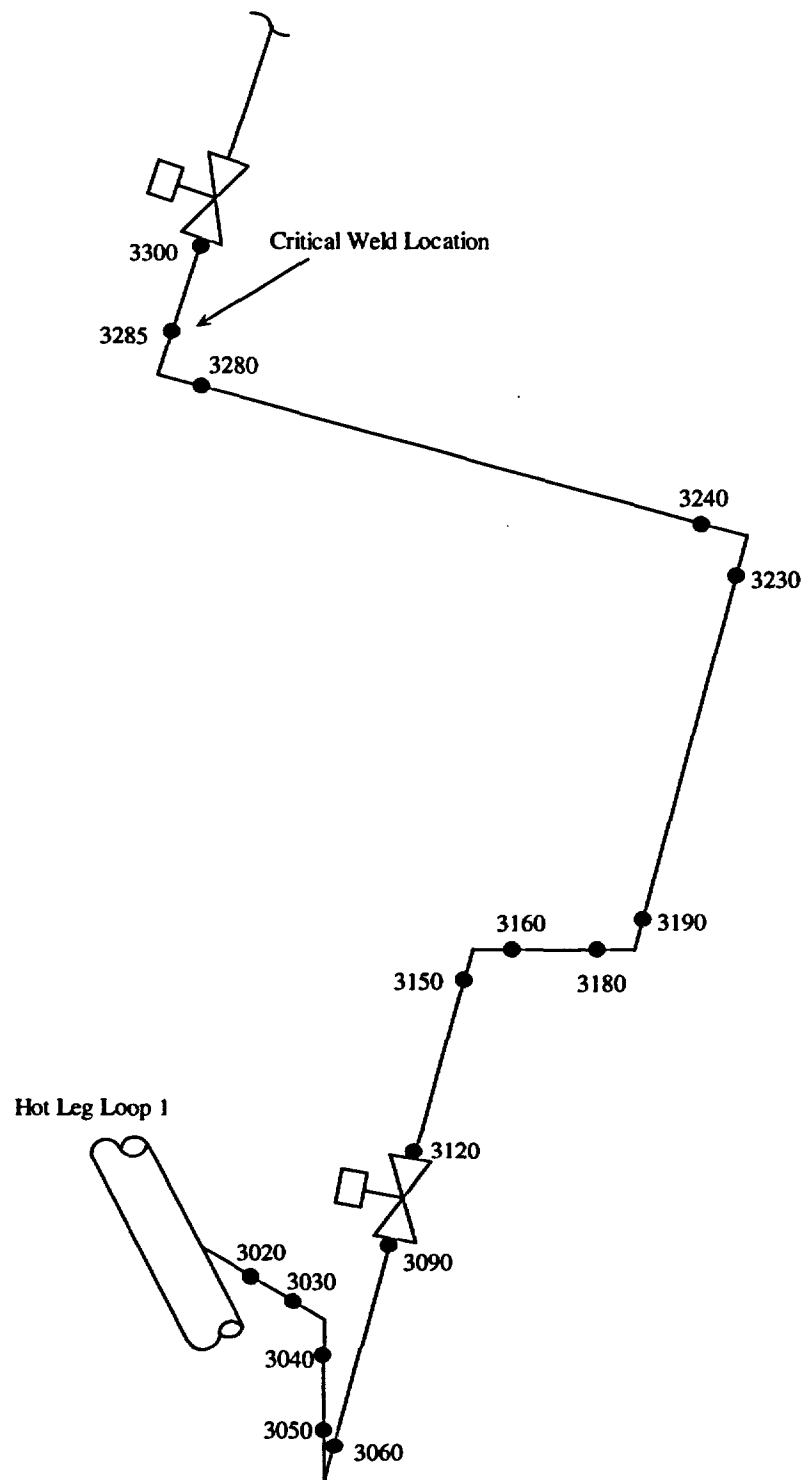


Figure 4-1 Governing Weld Location for RHR Line Loop 1

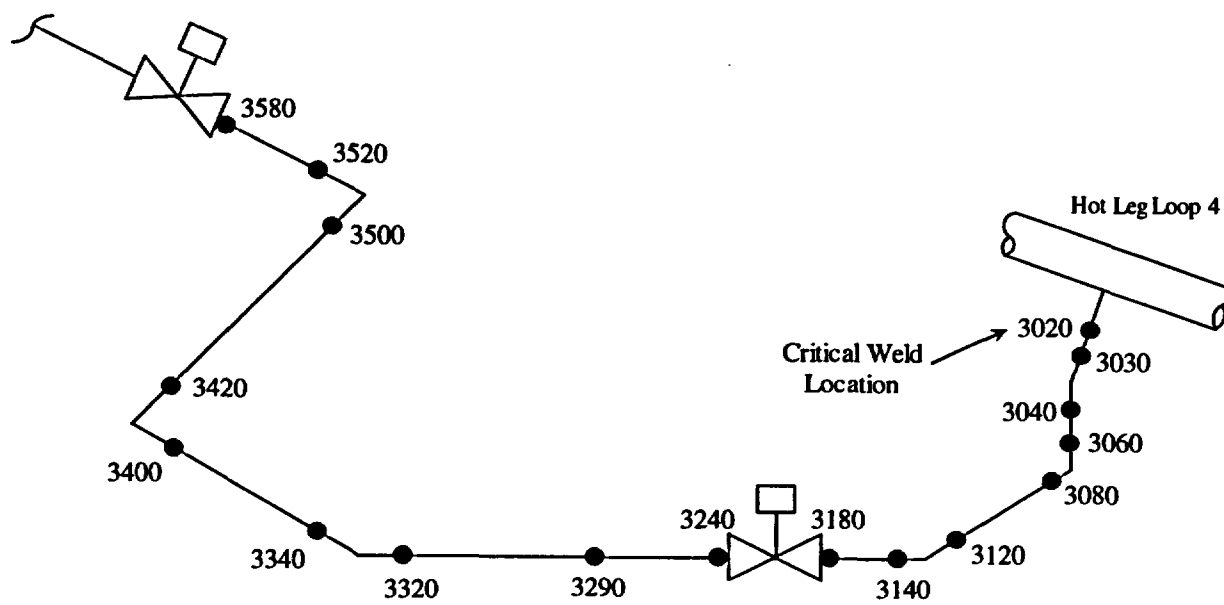


Figure 4-2 Governing Weld Location for RHR Line Loop 4

5 FRACTURE MECHANICS EVALUATION

5.1 GLOBAL FAILURE MECHANISM

Determination of the conditions, which lead, to failure in stainless steel should be done with plastic fracture methodology because of the large amount of deformation accompanying fracture. One method for predicting the failure of ductile material is the []^{a,c,e} method based on traditional plastic limit load concepts, but accounting for []^{a,c,e} and taking into account the presence of a flaw. The flawed component is predicted to fail when the remaining net section reaches a stress level at which a plastic hinge is formed. The stress level at which this occurs is termed as the flow stress. []

[]^{a,c,e} This methodology has been shown to be applicable to ductile piping through a large number of experiments and is used here to predict the critical flaw size in the RHR lines. The failure criterion has been obtained by requiring equilibrium of the section containing the flaw (Figure 5-1) when loads are applied. The detailed development is provided in Appendix A for a through-wall circumferential flaw in a pipe section with internal pressure, axial force, and imposed bending moments. The limit moment for such a pipe is given by:

$$[]^{a,c,e} \quad (5-1)$$

where:

[]

$$]^{a,c,e} \quad (5-2)$$

The analytical model described above accurately accounts for the internal pressure as well as the imposed axial force as they affect the limit moment. Good agreement was found between

the analytical predictions and the experimental results (Reference 5-1). The flaw stability evaluations using this analytical model are presented in Section 5.3.

5.2 LEAK RATE PREDICTIONS

Fracture mechanics analysis shows that postulated through-wall cracks in the RHR lines would remain stable and would not cause a gross failure of this component. However, if such a through-wall crack did exist, it would be desirable to detect the leakage such that the plant could be brought to a safe shutdown condition. The purpose of this section is to discuss the method, which will be used to predict the flow through such a postulated crack and present the leak rate calculation results for through-wall circumferential cracks.

5.2.1 General Considerations

The flow of hot pressurized water through an opening to a lower back pressure (causing choking) is taken into account. For long channels where the ratio of the channel length, L , to hydraulic diameter, D_H , (L/D_H) is greater than $[]^{a,c,e}$, both $[]^{a,c,e}$ must be considered. In this situation, the flow can be described as being single-phase through the channel until the local pressure equals the saturation pressure of the fluid. At this point, the flow begins to flash and choking occurs. Pressure losses due to momentum changes will dominate for $[]^{a,c,e}$. However, for large L/D_H values, the friction pressure drop will become important and must be considered along with the momentum losses due to flashing.

5.2.2 Calculation Method

In using the $[]^{a,c,e}$.

The flow rate through a crack was calculated in the following manner. Figure 5-2 from Reference 5-2 was used to estimate the critical pressure, P_c , for the primary loop enthalpy condition and an assumed flow. Once P_c was found for a given mass flow, the $[]^{a,c,e}$ was found from Figure 5-3 taken from Reference 5-2.

For all cases considered, since $[]^{a,c,e}$ Therefore, this method will yield the two-phase pressure drop due to momentum effects ($\Delta P_{2\phi}$) as illustrated in Figure 5-4. Now using the assumed flow rate, G , the frictional pressure drop can be calculated using

$$\Delta P_F = []^{a,c,e} \quad (5-3)$$

where the friction factor f was determined using the []^{a,c,e} The crack relative roughness, ϵ , was obtained from fatigue crack data on stainless steel samples. The relative roughness value used in these calculations was []^{a,c,e} RMS.

The frictional pressure drop using Equation 5-3 was then calculated for the assumed flow and added to the []^{a,c,e} to obtain the total pressure drop from the system under consideration to the atmosphere. Thus,

$$\text{Absolute Pressure} - 14.7 = []^{\text{a,c,e}} \quad (5-4)$$

for a given assumed flow G . If the right-hand side of Equation 5-4 does not agree with the pressure difference between the piping under consideration and the atmosphere, then the procedure is repeated until Equation 5-4 is satisfied to within an acceptable tolerance and this results in the flow value through the crack.

For the locations at the lower temperatures, the leak rate is calculated by using the simple orifice type flow formula given by []

$$(5-5)$$

$$]^{\text{a,c,e}}$$

5.2.3 Leak Rate Calculations

Leak rate calculations were performed as a function of postulated through-wall crack length for the governing locations previously identified. The crack opening area was estimated using the method of Reference 5-4 and the leak rates were calculated using the calculation methods described above. The leak rates were calculated using the normal operating loads at the governing locations identified in Section 4. Average yield strength properties from Table 3-2 were used in the leak rate calculations. The crack lengths yielding a leak rate of 10 gpm (10 times the leak detection capability of 1.0 gpm) for the governing locations at the Callaway Nuclear Power Plant RHR lines are shown in Table 5-1.

The Callaway Nuclear Power Plant has an RCS pressure boundary leak detection system which is consistent with the guidelines of Regulatory Guide 1.45 for detecting leakage of 1 gpm in one hour.

5.3 STABILITY EVALUATION

A typical segment of the pipe under maximum loads of axial force F and moment M is schematically illustrated in Figure 5-5. In order to calculate the critical flaw size, plots of the limit moment versus crack length are generated as shown in Figures 5-6 to 5-7. The critical flaw size corresponds to the intersection of this curve and the maximum load line. The critical flaw size is calculated using the lower bound base metal tensile properties tabulated in Table 3-2.

The weld process types for all the shop welds and field welds are Gas Tungsten Arc Weld (GTAW) and Shielded Metal Arc Weld (SMAW) combination or GTAW. Although the weld process at the critical weld locations identified in Section 4.5 is GTAW, in order to envelop all the weld process types in the stability evaluation, SMAW weld process type is conservatively assumed. Therefore, the "Z" factor correction for the SMAW was applied (Reference 5-5) as follows:

$$Z = 1.15 [1 + 0.013 (OD - 4)] \quad (\text{for SMAW}) \quad (5-6)$$

where OD is the outer diameter in inches. Substituting $OD = 12.75$ inches, the Z factor was calculated to be 1.28 for SMAW. The "Z" correction factor for GTAW is 1.0. The applied loads were increased by the Z factors for SMAW and the plots of limit load versus crack length were generated as shown in Figures 5-6 to 5-7 for the critical locations. Table 5-2 shows the summary of critical flaw sizes.

5.4 REFERENCES

- 5-1 Kanninen, M. F. et al., "Mechanical Fracture Predictions for Sensitized Stainless Steel Piping with Circumferential Cracks" EPRI NP-192, September 1976.
- 5-2 [

$\frac{1}{\sqrt{1 + \frac{1}{2} \left(\frac{a}{c} \right)^2}}$
- 5-3 Crane, D.P., "Handbook of Hydraulic Resistance Coefficient."
- 5-4 Tada, H., "The Effects of Shell Corrections on Stress Intensity Factors and the Crack Opening Area of Circumferential and a Longitudinal Through-Crack in a Pipe," Section II-1, NUREG/CR-3464, September 1983.
- 5-5 Standard Review Plan; Public Comment Solicited; 3.6.3 Leak-Before-Break Evaluation Procedures; Federal Register/Vol. 52, No. 167/Friday, August 28, 1987/Notices, pp. 32626-32633.

Table 5-1 : Leakage Flaw Sizes

Node Point	Temperature (°F)	Crack Length (in.) (for 10 gpm leakage)
3020	619	3.41
3285	70	2.97

Table 5-2 : Summary of Critical Flaw Sizes

Node Point	Temperature (°F)	Critical Flaw Size (in)
3020	619	10.25
3285	70	12.99

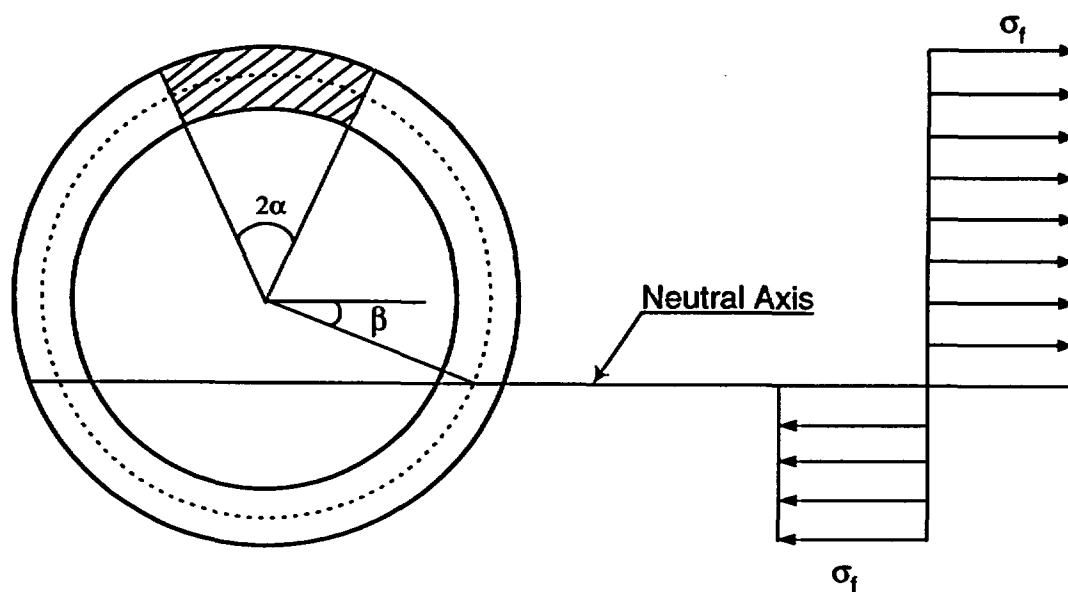


Figure 5-1 Fully Plastic Stress Distribution

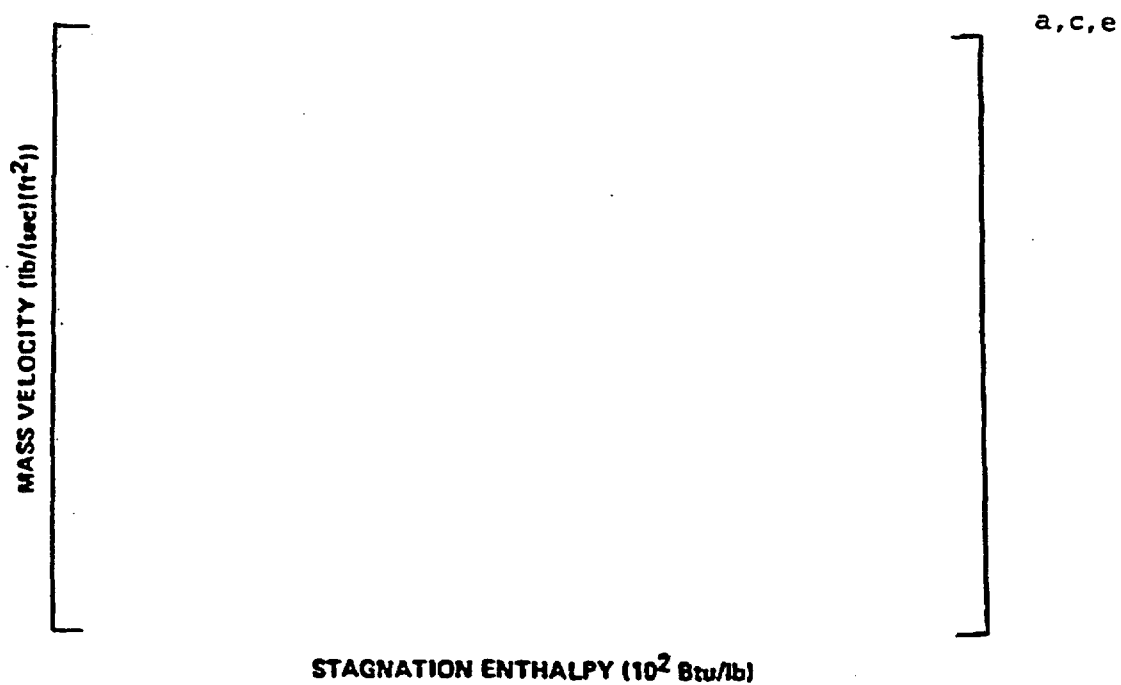


Figure 5-2 Analytical Predications of Critical Flow Rates of Steam-Water Mixtures

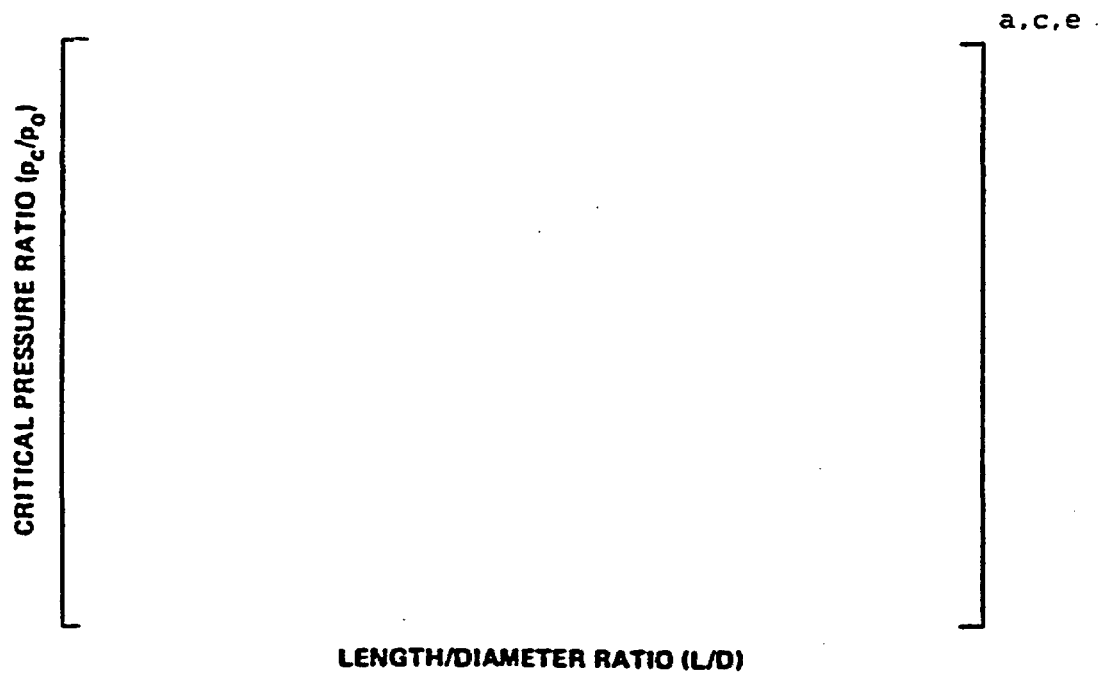


Figure 5-3 [

]a, c, e Pressure Ratio as a Function of L/D

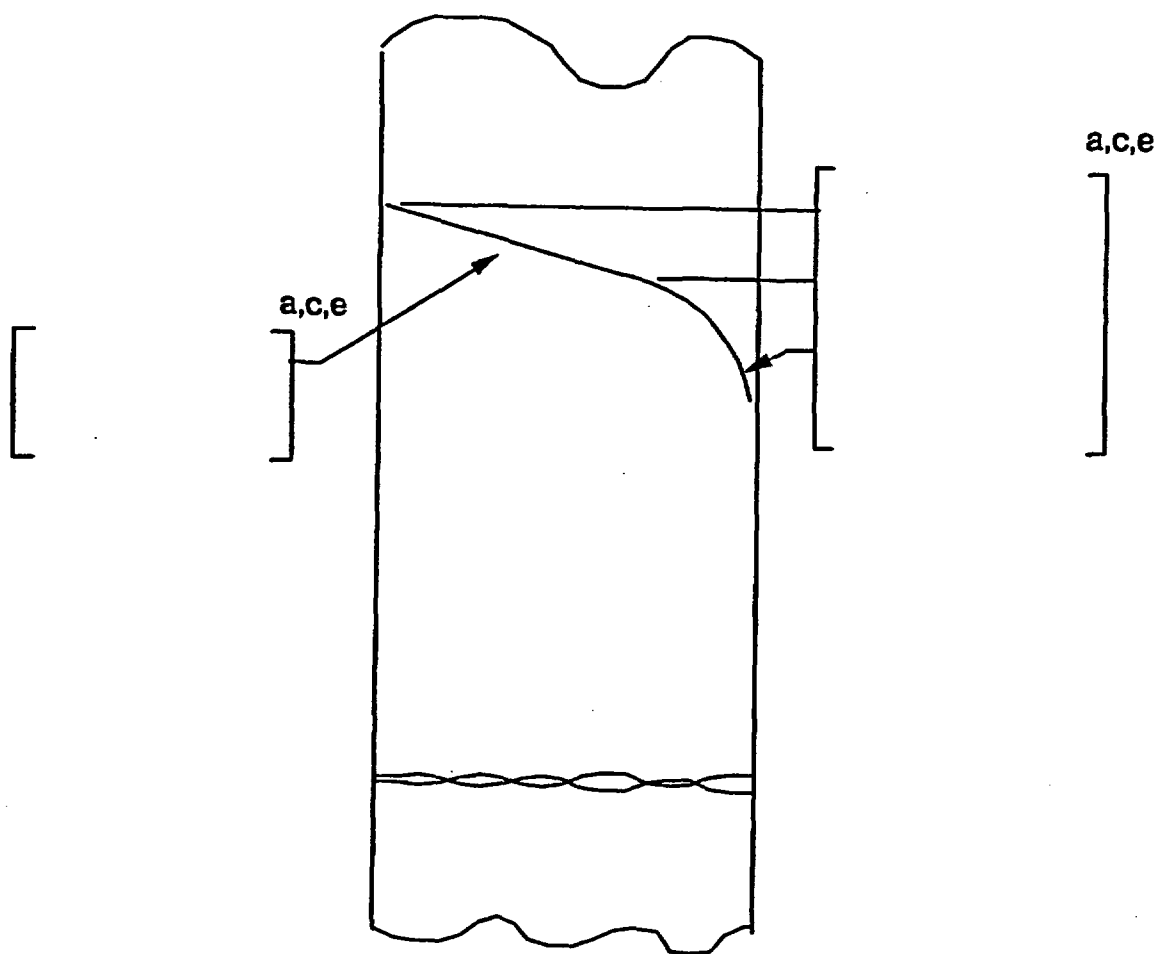


Figure 5-4 Idealized Pressure Drop Profile through a Postulated Crack

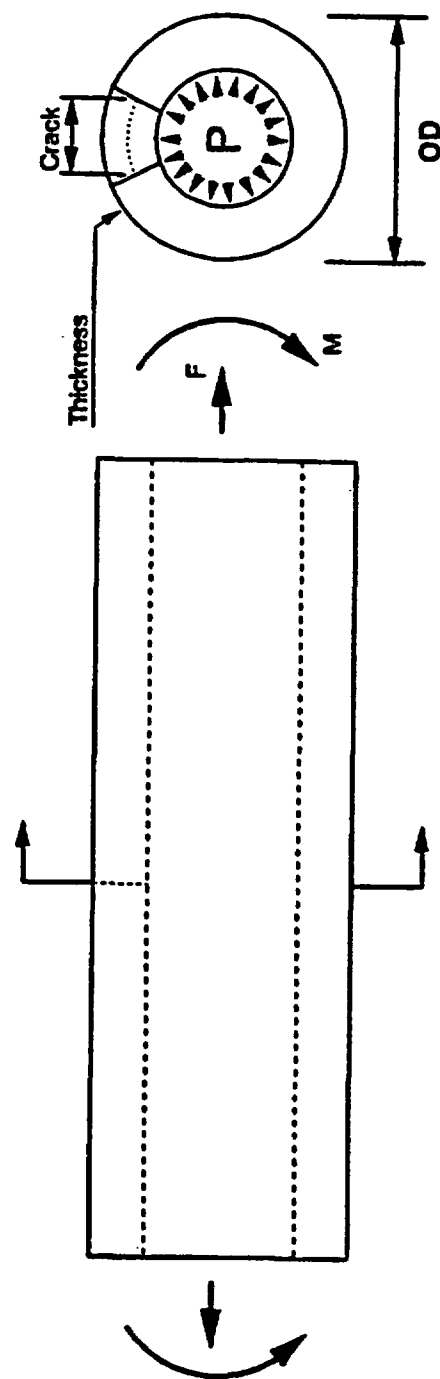


Figure 5-5 Loads acting on the Model at the Governing Locations



OD = 12.75 in $\sigma_y = 22.384$ ksi F = 232.496 kips
t = 1.005 in $\sigma_u = 68.244$ ksi M = 1826.562 in-kips
SA376/SA312 TP304 or SA403 WP304 with SMAW weld

Figure 5-6 Critical Flaw Size Prediction for Node 3020 (RHR Line Loop 4)



OD = 12.75 in $\sigma_y = 36.800$ ksi F = 228.015 kips
t = 1.005 in $\sigma_u = 80.730$ ksi M = 1751.544 in-kips
SA376/SA312 TP304 or SA403 WP304 with SMAW weld

Figure 5-7 Critical Flaw Size Prediction for Node 3285 (RHR Line Loop 1)

6 ASSESSMENT OF FATIGUE CRACK GROWTH

6.1 INTRODUCTION

The fatigue crack growth of the Callaway Nuclear Power Plant RHR lines was determined by comparison with a generic fatigue crack growth analysis of a similar piping system. The details of the generic fatigue crack growth analysis are presented below. By comparing all parameters critical to the fatigue crack growth analysis between Callaway and the generic analysis, it was concluded that the generic analysis would adequately cover the fatigue crack growth of the Callaway Nuclear Power Plant RHR lines.

Due to similarities in Westinghouse PWR designs, it was possible to perform a representative fatigue crack growth calculation which would be applicable to the Callaway Nuclear Power Plant. A comparison was made of the number of cycles, material, geometry, and types of discontinuities.

6.2 CRITICAL LOCATION FOR FATIGUE CRACK GROWTH ANALYSIS

The weld locations at the RCL hot leg nozzles to RHR lines (see Figures 3-1 and 3-2) were determined to be the most critical location for the fatigue crack growth evaluation. The nozzle configuration and weld location is shown in Figure 6-1. The geometry of the pipe was identical between the Callaway Nuclear Power Plant and the generic model (12" Schedule 140). Both analyses used austenitic stainless steel at the critical location.

6.3 DESIGN TRANSIENTS

The transient conditions selected for this evaluation are based on conservative estimates of the magnitude and the frequency of the temperature fluctuations documented in various operating plant reports. These are representative of the conditions which are considered to occur during plant operation. The normal operating and upset thermal transients, in accordance with the design specification and the applicable system design criteria document, were considered for this evaluation. Out of these, 20 transients were used in the fatigue crack growth analysis and are listed in Table 6-1. There are some differences between the generic transients used in the fatigue crack growth evaluation and the Callaway Nuclear Power Plant transients but these differences would have insignificant impact on the fatigue crack growth results.

6.4 STRESS ANALYSIS

A thermal transient stress analysis was performed for a typical plant similar to the Callaway Nuclear Power Plant to obtain the through-wall stress profiles for use in the fatigue crack growth analysis. The generic RHR line design transients described in Section 6.3 were used.

A simplified analysis method was used to develop conservative maximum and minimum linear through wall stress distributions due to thermal transients. In this method, a 1-D computer program was used to perform the thermal analysis to determine the through wall temperature

gradients as a function of time. The inside surface stress was calculated by using an equation, which is similar to the transient portion of ASME Section III NB 3600, Equation (11). The effect of discontinuity was included in the analysis by performing a separate 1-D thermal analysis for the pipe and nozzle. The maximum and minimum inside surface stresses were then obtained by searching the inside surface stress values calculated for each time step of the transient solution. The outside surface stresses corresponding to the maximum and minimum inside surface stresses were then calculated by a similar method. The maximum and minimum linear through wall stress distribution for each thermal transient was obtained by joining the corresponding inside and outside surface stresses by a straight line. These two stress profiles are called the maximum and minimum through wall stress distributions respectively, for convenience. The stresses due to the generic pressure and the generic moment loading were then superimposed on the through wall cyclical stresses to obtain the total maximum and minimum stress profile for each transient.

6.5 OBE LOADS

The stresses due to OBE loads were neglected in the fatigue crack growth analysis since these loads are not expected to contribute significantly to crack growth due to the small number of cycles.

6.6 TOTAL STRESS FOR FATIGUE CRACK GROWTH

The total through wall stress at a section was obtained by superimposing the generic pressure stress and the generic moment stresses on the thermal transient stresses. Thus, the total stress for fatigue crack growth at any point is given by the following equation:

$$\begin{array}{ccccccc} \text{Total Stress} & & & & \text{Stress due to} & & \\ \text{For Fatigue} & & & & \text{Internal} & & \\ \text{Crack} & = & & + & \text{Moment (DW} & + & \text{Thermal} \\ \text{Growth} & & & & \text{+ Thermal} & & \text{Transient Stress} \\ & & & & \text{Expansion)} & & \end{array}$$

6.7 FATIGUE CRACK GROWTH ANALYSIS

The fatigue crack growth analysis was performed to determine the effect of the design thermal transients tabulated in Table 6-1. The analysis was performed for the critical cross-section identified in Figure 6-1. A range of crack depths was postulated, and each was subjected to the transients in Table 6-1, which included pressure and moment loads.

6.7.1 Analysis Procedure

The fatigue crack growth analyses presented herein were conducted in the same manner as suggested by Section XI, Appendix A of the ASME Boiler and Pressure Vessel Code (Reference 6-1). The analysis procedure involves assuming an initial flaw exists at some point and predicting the growth of that flaw due to an imposed series of transient stresses. The

growth of a crack per loading cycle is dependent on the range of applied stress intensity factor, ΔK_I , by the following:

$$\frac{da}{dN} = C_o \Delta K_I^n \quad (6-1)$$

where " C_o " and the exponent " n " are material properties, and ΔK_I is defined later. For inert environments these material properties are constants, but for some water environments they are dependent on the level of mean stress present during the cycle. This can be accounted for by adjusting the value of " C_o " by a function of the ratio of minimum to maximum stress for any given transient, as will be discussed later. Fatigue crack growth properties of stainless steel in a pressurized water environment have been used in the analysis.

The input required for a fatigue crack growth analysis is basically the information necessary to calculate the parameter ΔK_I , which depends on crack and structure geometry and the range of applied stresses in the area where the crack exists. Once ΔK_I is calculated, the growth due to that particular cycle can be calculated by Equation (6-1). This increment of growth is then added to the original crack size, the ΔK_I adjusted, and the analysis proceeds to the next transient. The procedure is continued in this manner until all the transients have been analyzed.

The applied stresses at the flaw locations are resolved into membrane and bending stresses with respect to the wall thickness. Pressure, thermal, and discontinuity stresses are considered in the determination of the K_I factors.

The stress intensity factor at the point of maximum depth is calculated from the membrane and bending stresses using the following equation taken from the ASME Code (Reference 6-1):

$$K_I = \sqrt{\frac{\pi a}{Q}} [\sigma_m M_m + \sigma_b M_b]$$

where : σ_m, σ_b = Membrane and Bending Stress, respectively

a = Minor Semi-Axis (flaw depth)

Q = Flaw Shape Parameter Including A Plastic Zone Correction Factor for Plane Strain Condition

Q = $[\phi_1^2 - 0.212 (\sigma / \sigma_{ys})^2]$

ϕ_1 = $\int_0^{\pi/2} \left[1 - \left(\frac{b^2 - a^2}{b^2} \right) \cos^2 \Phi \right]^{1/2} d\Phi$

σ_{ys} = Yield Strength of the Material

$$\sigma = \sigma_m + \sigma_b$$

$$b = \text{Major Semi-Axis (Flaw Length/2)}$$

$$\phi = \text{Parametric Angle of the Ellipse}$$

$$M_m = \text{Correction Factor for Membrane Stress}$$

$$M_b = \text{Correction Factor for Bending Stress}$$

The appropriate values of M_m and M_b as a function of crack geometry can be found in Reference 6-1. The range of stress intensity factor (ΔK_I) for fluctuation of applied stress is determined by first finding the maximum and minimum stress intensity factor ($K_{I \max}$, $K_{I \min}$) during a given transient and then calculating the range of stress intensity factor ($\Delta K_I = K_{I \max} - K_{I \min}$). At times $K_{I \min}$ may go below zero, in these cases, $K_{I \min}$ is set equal to zero before ΔK_I is determined.

Calculation of the fatigue crack growth for each cycle was then carried out using the reference fatigue crack growth rate law determined from consideration of the available data for stainless steel in a pressurized water environment. This law allows for the effect of mean stress or R ratio ($K_{I \min}/K_{I \max}$) on the growth rates.

The reference crack growth law used for the stainless steel RHR pipe system was taken from that developed by the Metal Properties Council - Pressure Vessel Research Committee Task Force In Crack Propagation Technology. The reference curve has the equation:

$$[\quad] \quad (6-2)$$

$$]^{a,c,e}$$

This equation appears in Appendix C of ASME Section XI for air environments and its basis is provided in Reference 6-2, and shown in Figure 6-2. For water environments, an environmental factor of $[\quad]^{a,c,e}$ was used, based on the crack growth tests in PWR environments reported in Reference 6-3.

6.8 RESULTS

Fatigue crack growth analyses were carried out at the critical cross-section. Analysis was completed for a range of postulated flaw sizes oriented circumferentially, and the results are presented in Table 6-2. The postulated flaws are assumed to have an aspect ratio of six to one. Even for the largest postulated flaw of 0.35 inch, which is about 35 percent of the wall thickness, the result projects that the flaw growth through the wall will not occur during the 40 year design life of the plant. Therefore, fatigue crack growth should not be a concern for the Callaway Nuclear Power Plant RHR Lines.

6.9 REFERENCES

- 6-1 ASME Boiler and Pressure Vessel Code Section XI, 2001 Edition, "Rules for Inservice Inspection of Nuclear Power Plant Components"
- 6-2 James, L. A., and Jones, D. P., "Fatigue Crack Growth Correlations for Austenitic Stainless Steel in Air," in Predictive Capabilities in Environmentally Assisted Cracking, ASME publication PVP-99, Dec. 1985.
- 6-3 Bamford, W. H., "Fatigue Crack Growth of Stainless Steel Piping in a Pressurized Water Reactor Environment," Trans ASME, Journal of Pressure Vessel Technology, Feb. 1979. Engineering Development Labs Report HEDL-TME-76-43, May 1976.

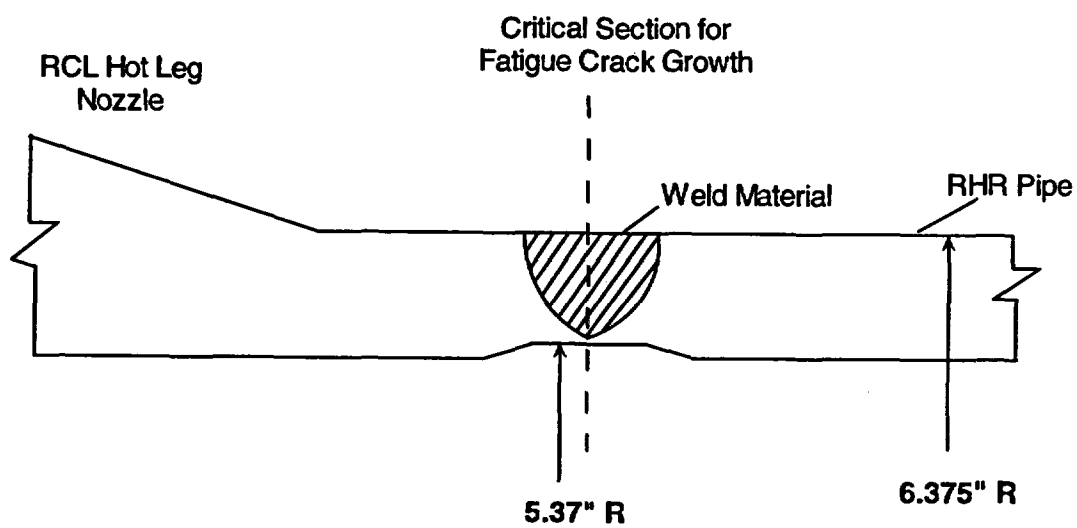
Table 6-1 : Design Transients Considered for Fatigue Crack Growth Evaluation .

Trans. No.	Description	No. of Occurrences
1	Unit Loading	13,200
2	Unit Unloading	13,200
3	Step Load Increase	2,000
4	Step Load Decrease	2,000
5	Large Step Load Decrease with Steam Dump	200
6	Feedwater Cycling	2000
7	Unit Loading Between 0 and 15% Power	500
8	Unit Unloading Between 0 and 15% Power	500
9	Loss of Load	80
10	Loss of Power	40
11	Partial Loss of Flow-Dead Loop	80
12	Partial Loss of Flow-Active Loop	80
13	Reactor Trip with no Inadvertent Cooldown	230
14	Reactor Trip with Cooldown; No Safety Injection	160
15	Reactor Trip with Cooldown Actuating Safety Injection	10
16	Inadvertent RCS Depressurization	20
17	Control Rod Drop	80
18	Inadvertent Safety Injection	60
19	Turbine Roll Test	20
20	Steady-State and Random Fluctuations	3.2×10^6

Table 6-2 : RHR Lines Fatigue Crack Growth Results

Initial	Crack Depth (in) After			

a,c,e



R is the pipe radius

Figure 6-1 Schematic of RHR Line at RCL Hot Leg Nozzle Weld Location

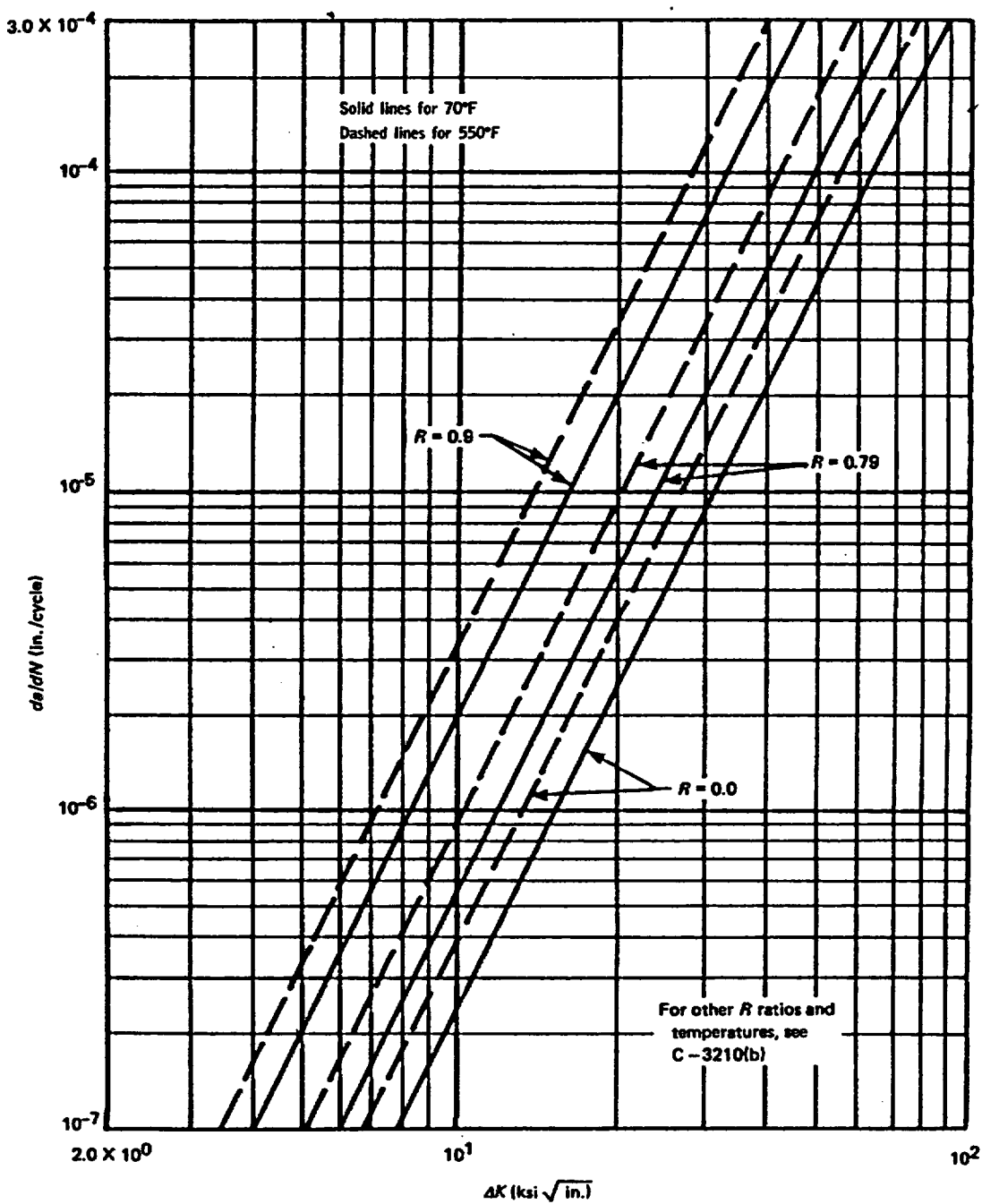


Figure 6-2 Reference Crack Growth Curves for Stainless Steel in Air Environments

7 ASSESSMENT OF MARGINS

In the preceding sections, the leak rates calculations, fracture mechanics analysis and fatigue crack growth assessment was performed.

The results of the leak rates of Section 5.2 and the corresponding stability results of Section 5.3 are used in performing the assessment of margins. Margins are shown in Table 7-1.

In summary, at all the critical locations relative to:

1. Flaw Size - Using faulted loads obtained by the absolute sum method, a margin of 2 or more exists between the critical flaw and the flaw having a leak rate of 10 gpm (the leakage flaw).
2. Leak Rate - A margin of 10 exists between the calculated leak rate from the leakage flaw and the leak detection capability of 1 gpm.
3. Loads - At the critical locations, the leakage flaw was shown to be stable using the faulted loads obtained by the absolute sum method (i.e., a flaw twice the leakage flaw size is shown to be stable; hence the leakage flaw size is stable). Therefore a margin on loads of 1.0 (see Section 4.2 for explanation) using the absolute summation of faulted load combinations is satisfied.

All the LBB recommended margins are satisfied.

In this evaluation, the Leak-Before-Break methodology is applied conservatively. The conservatism used in the evaluation is summarized in Table 7-2.

Table 7-1 : Leakage Flaw Sizes, Critical Flaw Sizes and Margins

Node	Critical Flaw Size (in)	Leakage Flaw Size (in)	Margin
3020	10.25	3.41	3.01
3285	12.99	2.97	4.37

Table 7-2 : LBB Conservatism

Factor of 10 on Leak Rate
Factor of 2 on Leakage Flaw
Algebraic Sum of Loads for Leakage
Absolute Sum of Loads for Stability
Average Material Properties for Leakage
Minimum Material Properties for Stability

8 CONCLUSIONS

This report justifies the elimination of RHR line pipe breaks as the structural design basis for the Callaway Nuclear Power Plant as follows:

- a. Stress corrosion cracking is precluded by use of fracture resistant materials in the piping system and controls on reactor coolant chemistry, temperature, pressure, and flow during normal operation.
- b. Water hammer should not occur in the RCS piping (primary loop and the attached class 1 auxiliary lines) because of system design, testing, and operational considerations.
- c. The effects of low and high cycle fatigue on the integrity of the RHR lines were evaluated and shown acceptable.
- d. Ample margin exists between the leak rate of small stable flaws and the capability of Callaway Nuclear Power Plant reactor coolant system pressure boundary leakage detection system.
- e. Ample margin exists between the small stable flaw sizes of item (d) and the critical flaw size.

The postulated reference flaw will be stable because of the ample margins in items (d) and (e) and will leak at a detectable rate which will assure a safe plant shutdown.

Based on the above, it is concluded that RHR line breaks should not be considered in the structural design basis of the Callaway Nuclear Power Plant.

APPENDIX A - LIMIT MOMENT

[

j_{a,c,e}

a,c,e



Figure A-1 Pipe with A Through-Wall Crack in Bending